

Appendix Table of Contents

This PDF file includes:

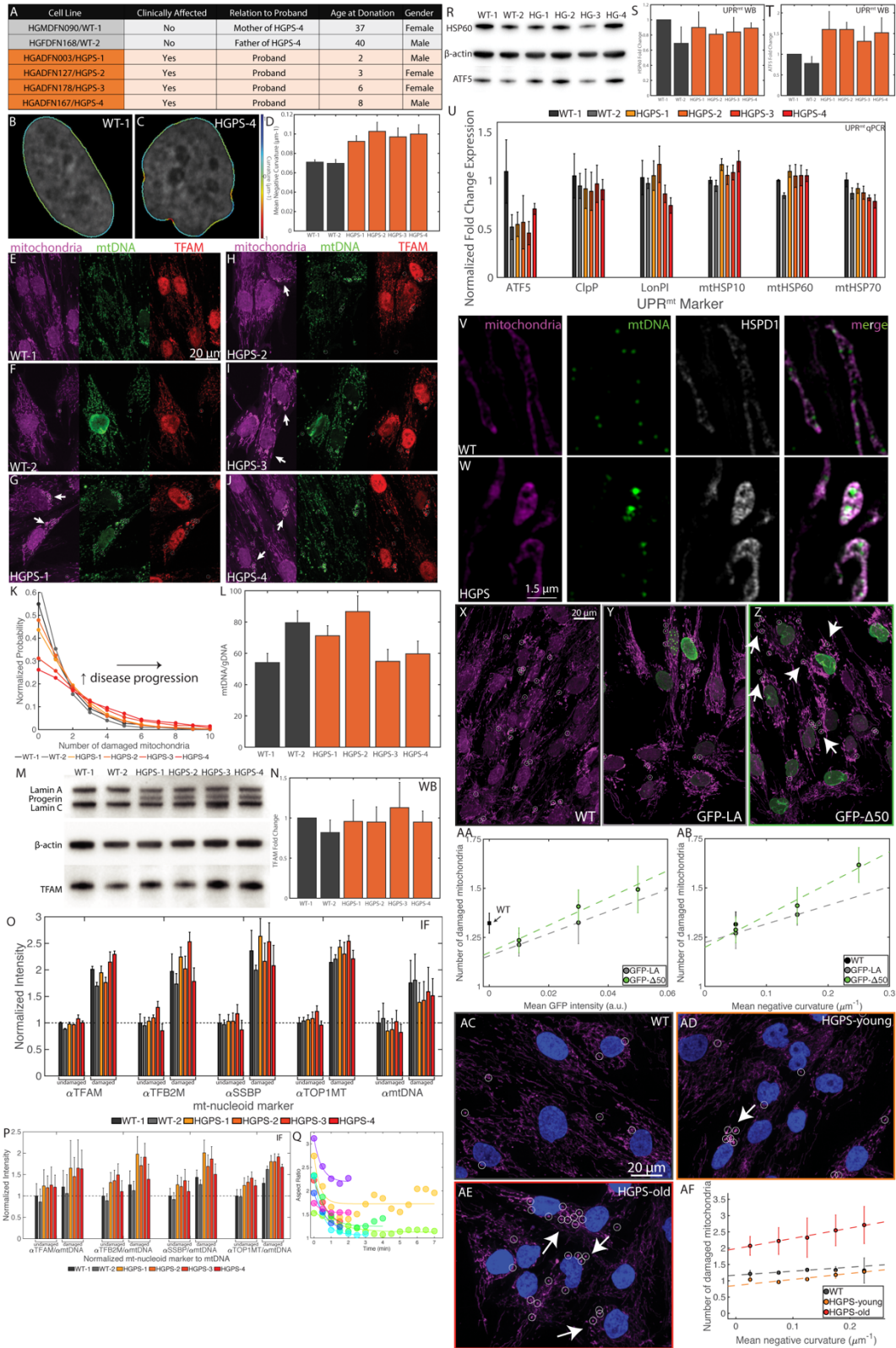
Appendix Table S1
Appendix Figures S1 to S7

Appendix Table S1: qPCR primers

qPCR target	Forward Primer	Reverse Primer
12S*	5'-ATGCAGCTCAAACGCTTAGC-3'	5'-GCTGGCACGAAATTGACCAA-3'
mtCOI*	5'-CAGCAGTCCTACTTCTCCTATCTCT-3'	5'-GGGTCGAAGAAGGTGGTGTT-3'
ACTB	5'-CATGTACGTTGCTATCCAGGC-3'	5'-CTCCTTAATGTCACGCACGAT-3'
ATF5†	5'-CTGGCTCCCTATGAGGTCCTTG-3'	5'-GAGCTGTGAAATCAACTCGCTCAG-3'
TUBB1	5'-CTACAACGCGGTTCTGTCTATC-3'	5'-GGTGGGTGTCGTCAGCTTC-3'
CLPP‡	5'-GCGCGCCTATGACATCTACT-3'	5'-AACGCTGTCATCGATCGGG-3'
LONP1‡	5'-CATGACGATCCCCGATGTGT-3'	5'-ACATCCGACTCATTGCTGTCA-3'
HSPE1 (mtHSP10)‡	5'-AGTAATGGCAGGACAAGCGT-3'	5'-ACTGGTTGAATCTCTCCACCC-3'
HSPD1 (mtHSP60)‡	5'-TGCTTCGGTTACCCACAGTC-3'	5'-ACTGTTCTTCCCTTTGGCCC-3'
HSPA9 (mtHSP70)‡	5'-ACAAGCAAAGGTGCTGGAGA-3'	5'-GGCATTCCAACAAGTCGCTC-3'
TBP	5'-GAGCCAAGAGTGAAGAACAGTC-3'	5'-GCTCCCCACCATATTCTGAATCT-3'

*Primers normalized to ACTB. †Primers normalized to TUBB1. ‡Primers normalized to TBP.

Appendix Figure S1:

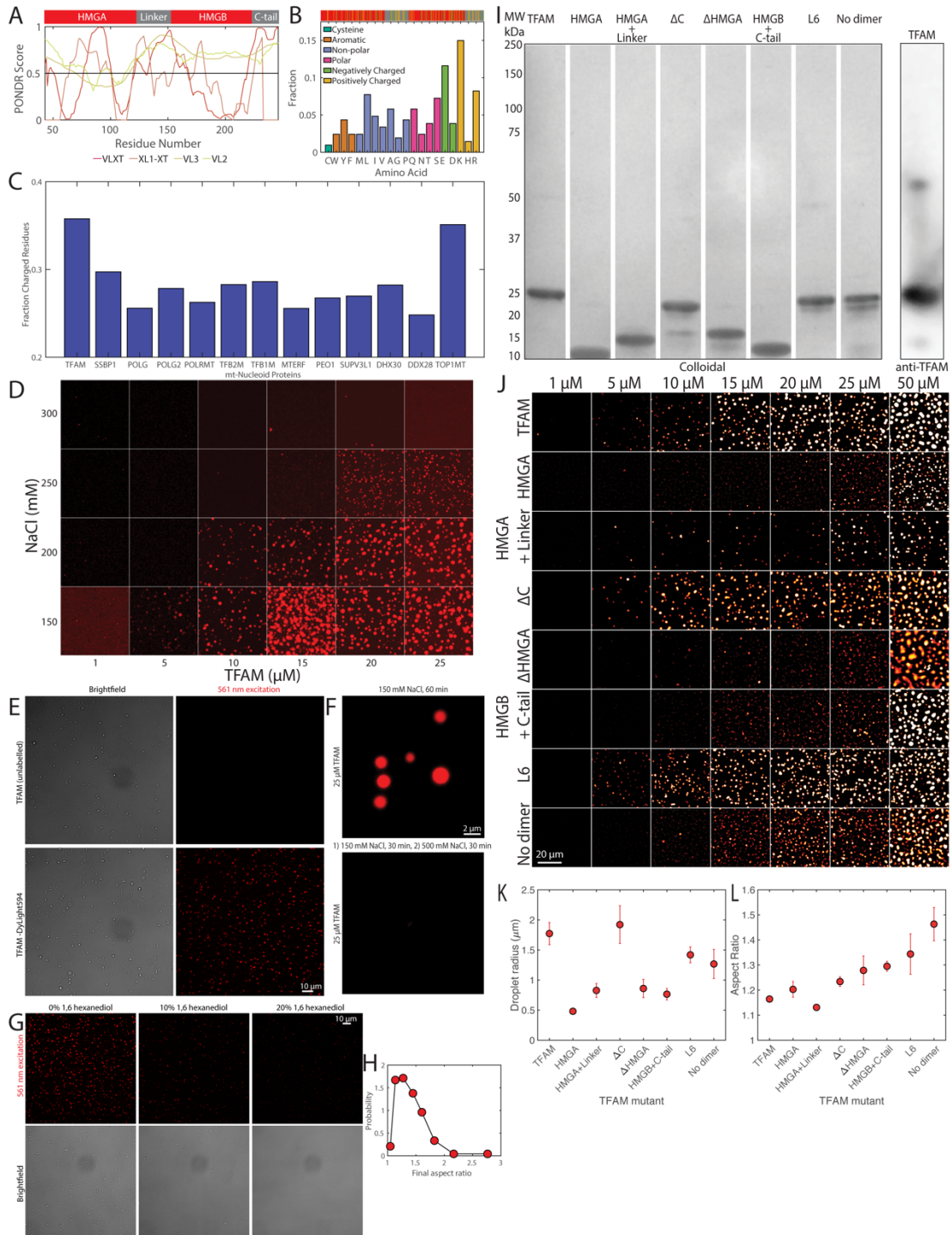


Appendix Figure 1: (A) Table summarizing primary skin fibroblast cell lines obtained from the Progeria Research Foundation (PRF). Categories included if patients are clinically affected with HGPS, their relation (if any), age at donation, and gender. (B-C) Images of typical segmentation of a nucleus exhibiting the normal, smooth phenotype from WT-1 cell line (B). or the irregular morphology from HGPS-4 cell line (C). Color scale shows curvature along the nuclear perimeter, where red = -1 and blue = 1. (D) Average mean negative curvature for all cell lines. Error bars represent standard deviation (where $n = 3$ experimental replicates, each with 8 technical replicates containing 5 fields of view. Approximately ~ 700 -3,000 cells analyzed per experimental replicate). (E-J) Representative high-throughput confocal images of WT-1 (E), WT-2 (F), HGPS-1 (G), HGPS-2 (H), HGPS-3 (I), and HGPS-4 (J) cell lines. Left image is mitochondria (MitoTracker Red, magenta); center image is mtDNA (anti-DNA, green); right image is TFAM (anti-TFAM, red). Scale bar = 20 μm . (K) Normalized probability distribution of number of damaged mitochondrial nucleoids for all cells of each primary cell line, which corresponds to data shown in Fig. 1C. (L) qPCR results of mtDNA copy number relative to genomic DNA for all cell lines tested, $n = 6$ experimental replicates and data are reported as mean \pm standard error. (M) Western blot results for all six primary cell lines showing bands for Lamin A, Progerin, and Lamin C as well as TFAM with B-actin as the housekeeping protein. (N) Quantification of TFAM protein levels from Western Blot in M, where $n = 6$ experimental replicates and data are reported as mean \pm standard error. (O) Based on high-throughput imaging, integrated intensity values for markers for nucleoid associated proteins (anti-TFAM, anti-TFB2M, anti-SSBP, and anti-TOP1MT) and anti-DNA were compared for nucleoids from undamaged and damaged mitochondria analyzed for each cell and averaged for all cells, where $n = 3$ experimental replicates and error bars represent standard error. (P) Average ratio of normalized nucleoid intensities from undamaged and damaged mitochondria on a per cell basis as a function of the mitochondrial marker (anti-TFAM, anti-TFB2M, anti-SSBP, and anti-TOP1MT). Normalization was done by taking the ratio of the integrated intensities of the protein marker over the respective mtDNA signal for each nucleoid, where $n = 3$ experimental replicates and error bars represent standard error.

(Q) Smoothed aspect ratio as a function of time for $n=8$ nucleoids after phototoxic stress, corresponding to experiments from Fig. 1H and 1I. Data was fit to single exponential decay to determine characteristic time scales; aspect ratio ≈ 1 , inverse capillary velocity $\approx 30 \pm 10$ s/micron, time scale $\approx 20 \pm 10$ s ($n=8$ nucleoids, error = s.e.m). (R) Western blot results for all six primary cell lines showing bands for UPR^{mt} markers anti-HSPD1 (mtHSP60) and ATF5 with B-actin as the housekeeping protein. (S) Quantification of HSPD1 (mtHSP60) protein levels from Western Blot in R, where $n = 3$ experimental replicates and data are reported as mean \pm standard error. (T) Quantification of ATF5 protein levels from Western Blot in R, where $n = 3$ experimental replicates and data are reported as mean \pm standard error ($p=0.3$). (U) qPCR results of UPR^{mt} markers (ATF5, ClpP, LonPI, mtHSP10, mtHSP60, mtHSP70) in all six primary cell lines reported as normalized fold change expression, where $n=3$ independent experimental replicates, each with three technical replicates, and error bars are standard error. (V-W) Representative z-slices of SIM images of WT (V) and HGPS (W) cell lines. Left image is mitochondria (MitoTracker Red, magenta); mtDNA (anti-DNA, green); HSPD1/mtHSP60 (anti-HSPD1, gray); right image is the merged image. Scale bar = 1.5 μ m. (X-Z) High-throughput confocal images of mitochondria from WT immortalized cells (X), GFP-lamin A (Y), and GFP-progerin (Z) with labelled mitochondria (MitoTracker Red, magenta) and GFP (green). Arrow heads point to GFP-progerin cells that exhibit the damaged mitochondrial phenotype observed in advanced HGPS cells. White circles indicate damaged mitochondria detected computationally. Scale bar = 20 μ m. (AA-AB) Number of damaged mitochondria as a function of mean GFP intensity (AA) and mean negative curvature (AB) for WT (black), GFP-lamin A (gray), and GFP-progerin (green). Cells were binned into equal bins, containing >50 cells per bin. Error bars are standard error for $n = 3$ experimental replicates, each with 9 technical replicates containing >16 fields of view (~ 600 - 3000 cells per experimental replicate for each cell line). Linear weighted fits are shown by dashed line. (AC-AE) High-throughput confocal images of mitochondria from WT primary cells (AC), HGPS-young primary cells (AD), and HGPS-old primary cells (AE) with labelled mitochondria (MitoTracker Red, magenta) and nuclei (DAPI, blue). Arrow heads point to HGPS cells that exhibit

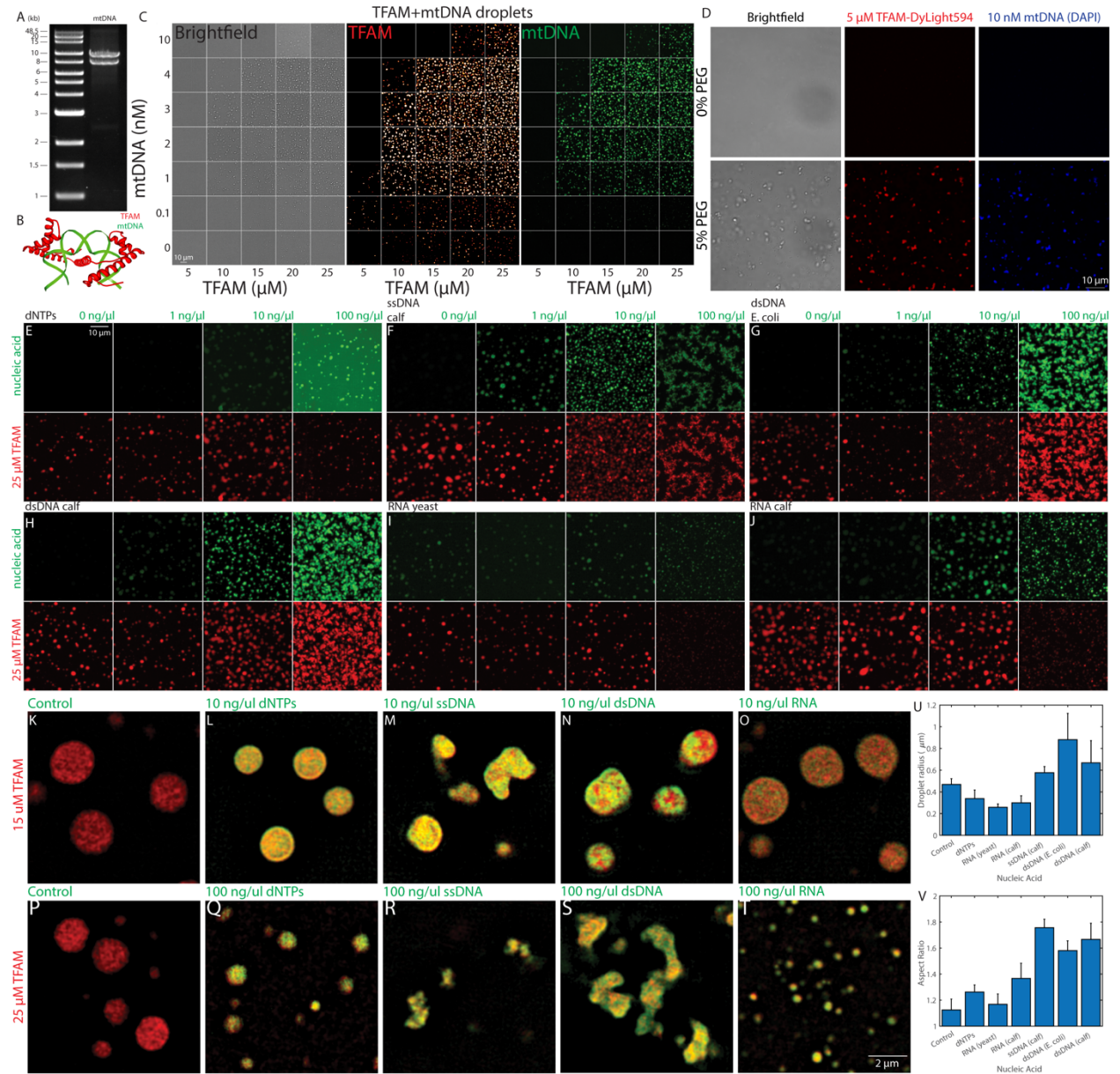
damaged mitochondrial phenotype. White circles indicate damaged mitochondria detected computationally. Scale bar = 20 μm . (AF) Number of damaged mitochondria as a function of mean negative curvature primary cells analyzed in Fig. 1. Cells were binned into equal bins, containing >50 cells per bin. Error bars are standard error for $n = 2$ experimental replicates, where primary cell lines have been grouped: WT (WT-1 and WT-2), HGPS-young (HGPS-1 and HGPS-2) and HGPS-old (HGPS-3 and HGPS-4). Each cell line has 8 technical replicates containing >5 fields of view (1500-4000 cells per experimental replicate for each cell line). Linear weighted fits are shown by dashed line.

Appendix Figure S2:



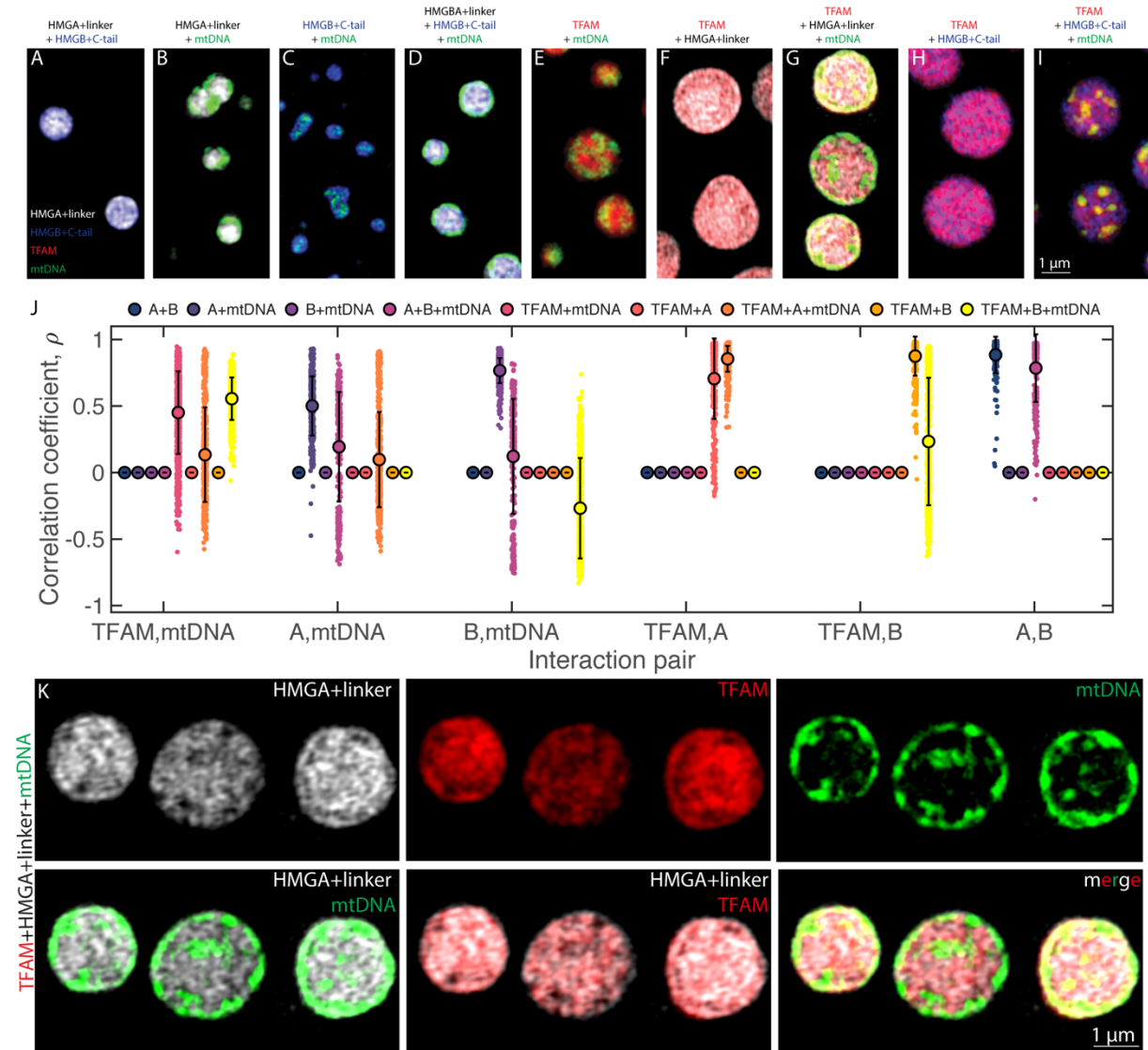
Appendix Figure S2: (A) PONDR score as a function of residue position of full length TFAM using the VLXT, XL1-XT, VL3, and VL2 algorithms. Top protein domain diagram shows corresponding functional domains with HMGs in red and disordered domains in grey. (B) Frequency of amino acids in full length TFAM. Top protein domain diagram shows position of negatively charged (green) and positively charged (yellow) residues. (C) Fraction of charged residues of core proteins in the mitochondrial nucleoid proteome involved in replication and transcription. (D) Images from a representative high-throughput microscopy experiment used to generate the phase diagram in Fig. 2A. Scale bar = 20 μm . (E) Effect of DyLight-594 labelling on droplet formation of TFAM. Top row is unlabelled TFAM at 25 μM and bottom row is DyLight-594 labelled 25 μM TFAM at $\sim 1:100$ ratio. Left column is brightfield image and right column is 561 channel. Scale bar = 10 μm . (F) Reversibility of phase separation experiment. Left panel shows contents after 60 minutes post mixing at 25 μM TFAM and 150 mM NaCl (Sample 1). Right panel shows contents from Sample 1 30 minutes after mixing followed by an additional 30 minutes in high salt buffer to reach 25 μM TFAM in 500 mM NaCl (Sample 2). Scale bar = 2 μm . (G) Effect of 1,6 hexanediol on droplet formation of TFAM. Top row is 561 nm excitation and bottom row is brightfield. Left column is untreated 25 μM TFAM, middle column is 10% 1,6 hexanediol, and right column is 20% 1,6 hexanediol at 20 mM Tris, 150 mM NaCl, pH 7.5. Scale bar = 10 μm . (H) Probability distribution of the aspect ratio upon completion of the fusion events observed in Fig. 2F. (I) Protein purification results. Left panel shows gel using Colloidal Blue Stain of purified full length TFAM and mutants. Right panel shows Western blot using anti-TFAM to confirm specificity of protein. (J) Images from high-throughput microscopy experiment used to generate the phase diagram and images in Fig. 2F,2G for TFAM and mutants ranging in concentration from 1, 5, 10, 15, 20, 25 and 50 μM . Scale bar = 20 μm . (K, L) Quantification of (K) average droplet radius or (L) final aspect ratio as a function of TFAM variants at 25 μM measured from three independent high-throughput imaging experiments, each with 12 fields of view ($n=3$, error bars = s.e.m.).

Appendix Figure S3:



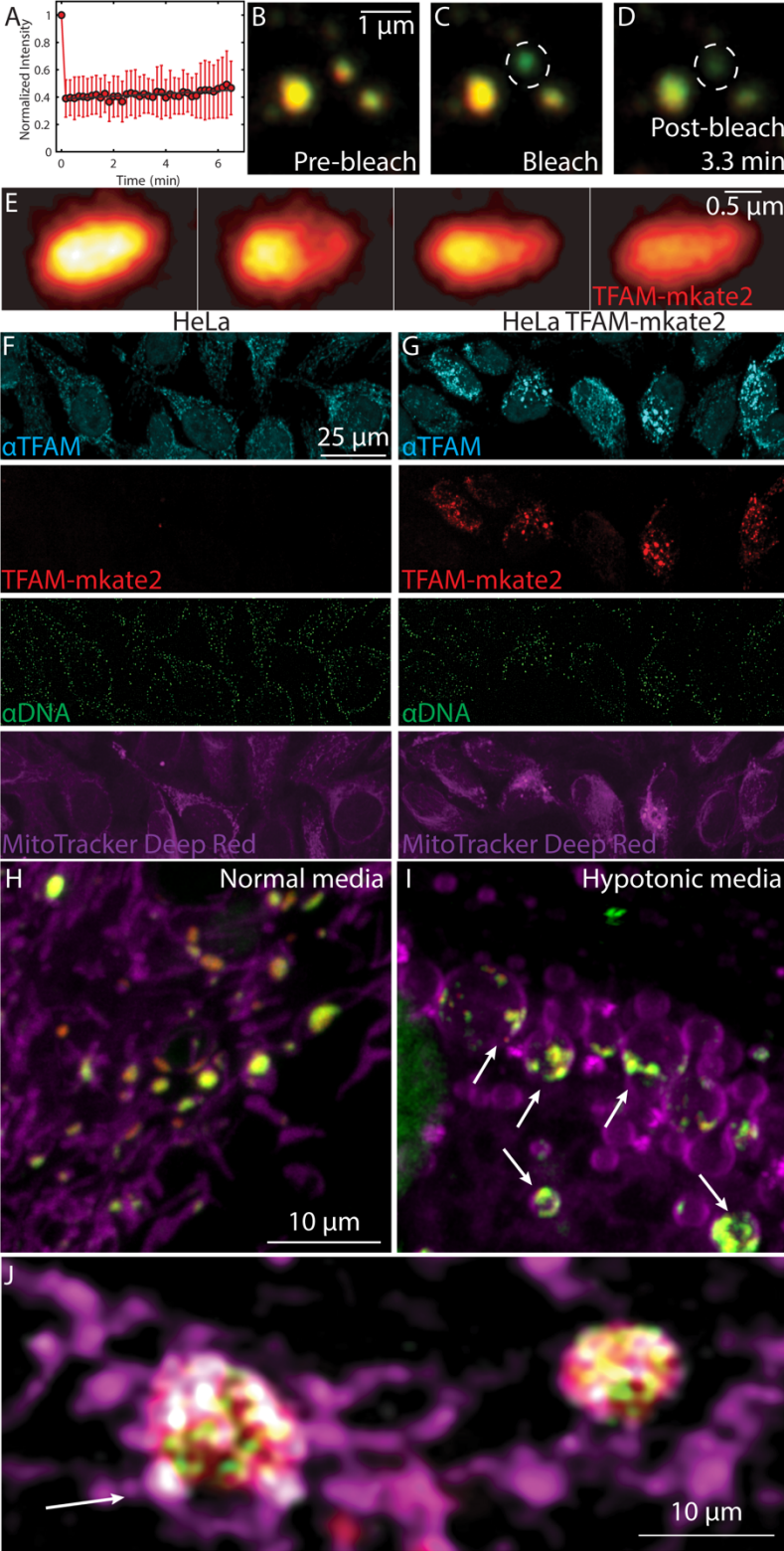
Appendix Figure S3: (A) Agarose gel stained with Ethidium Bromide showing purification of two mtDNA fragments (~7 and ~9 kb) after long-range PCR. (B) Cartoon illustrating TFAM-mtDNA binding based on structure obtained from X-ray crystallography. Adapted from Protein Data Base (see Methods). (C) An example high-throughput imaging assay of droplet formation upon various TFAM and mtDNA concentrations, indicated by brightfield, TFAM localization in red heat map, and mtDNA localization in green (labeled with dUTP-Alexa488). (D) Droplet formation upon 0% or 5% PEG (MW ~3K) at 5 μ M TFAM and 10 nM mtDNA (labelled with DAPI). (E-J) High-throughput images of nucleic acid addition to TFAM droplets. 25 μ M TFAM (final) was mixed with nucleic acids containing 0, 1, 10, and 100 ng/ μ l (final) of dNTPs (E), ssDNA from calf (F), dsDNA from *E. coli* (G), dsDNA from calf (H), RNA from yeast (I), and RNA from calf (J). Top row is of the nucleic acids labelled with SYBR Gold or of dNTPs with dUTP-Alexa488, and bottom row contains droplets labelled with TFAM-Dylight594. Scale bar = 10 μ m. Intensities were matched across the conditions within each panel. (K-T), SIM images of TFAM (red) droplets mixed with various nucleic acids (green). (K-O) are at 15 μ M TFAM, where K = control, L = 10 ng/ μ l dNTPs, M = 10 ng/ μ l ssDNA calf, N = 10 ng/ μ l dsDNA calf, and O = 10 ng/ μ l RNA calf. (P-T) 25 μ M TFAM, where P = control, Q = 100 ng/ μ l dNTPs, R = 100 ng/ μ l ssDNA calf, S = 100 ng/ μ l dsDNA calf, and T = 100 ng/ μ l RNA calf. Scale bar = 2 μ m. (U) Droplet radius as a function of nucleic acid added, where n = 3 experimental replicates and error bars represent standard error of the mean. (V) Aspect ratio of droplets as a function of nucleic acid added, where n = 3 experimental replicates and error bars represent standard error of the mean.

Appendix Figure S4:



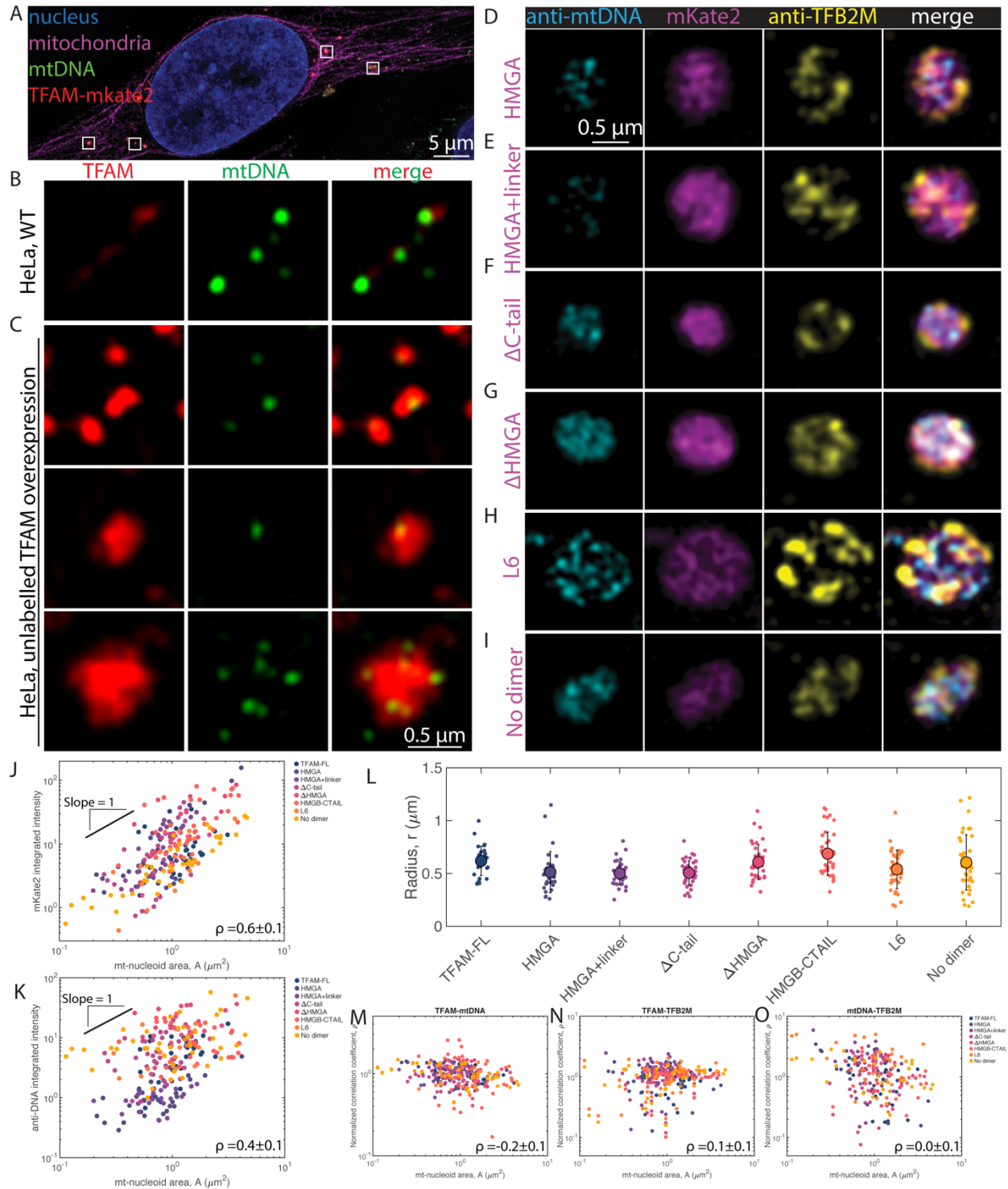
Appendix Figure S4: (A-I) Single z-slices of SIM images of various combinations of TFAM mutants with mtDNA, comprised of TFAM full length (red), HMGA+linker (gray-scale), HMGB+C-tail (blue), and/or mtDNA (green). Combinations are as follows: HMGA+linker and HMGB+C-tail (A), HMGA+linker and mtDNA (B), HMGB+C-tail and mtDNA (C), HMGA+linker, HMGB+C-tail and mtDNA (D), TFAM and mtDNA (E), TFAM and HMGA+linker (F), TFAM, HMGA+linker, and mtDNA (G), TFAM and HMGB+C-tail (H), and TFAM, HMGB+C-tail, and mtDNA (I). Scale bar = 1 μm . Final concentrations of TFAM mutants and mtDNA were 25 μM and ~ 1 nM, respectively. Scale bar = 1 μm . (J) Correlation coefficient as a function of each combination of TFAM mutants and mtDNA analyzed for multiple images (each small point on the graph is the measurement from a single droplet) obtained from experiments in (A-E). Large points represent average and error bars represent standard deviation, where $n = \sim 200$ -1000 droplets per condition. Note, HMGA+linker is abbreviated as A, and HMGB+C-tail is abbreviated as B. (K) Single z-slices of SIM images of compound droplets containing HMGA+linker (gray scale), TFAM (red), and mtDNA (green). Top row contains individual channels for HMGA+linker, TFAM, and mtDNA, respectively. Bottom panel shows overlays, where the left most is of HMGA+linker and mtDNA channels, middle panel is HMGA+linker and TFAM, and right most panel is the three-color overlay. Scale bar = 1 μm .

Appendix Figure S5:



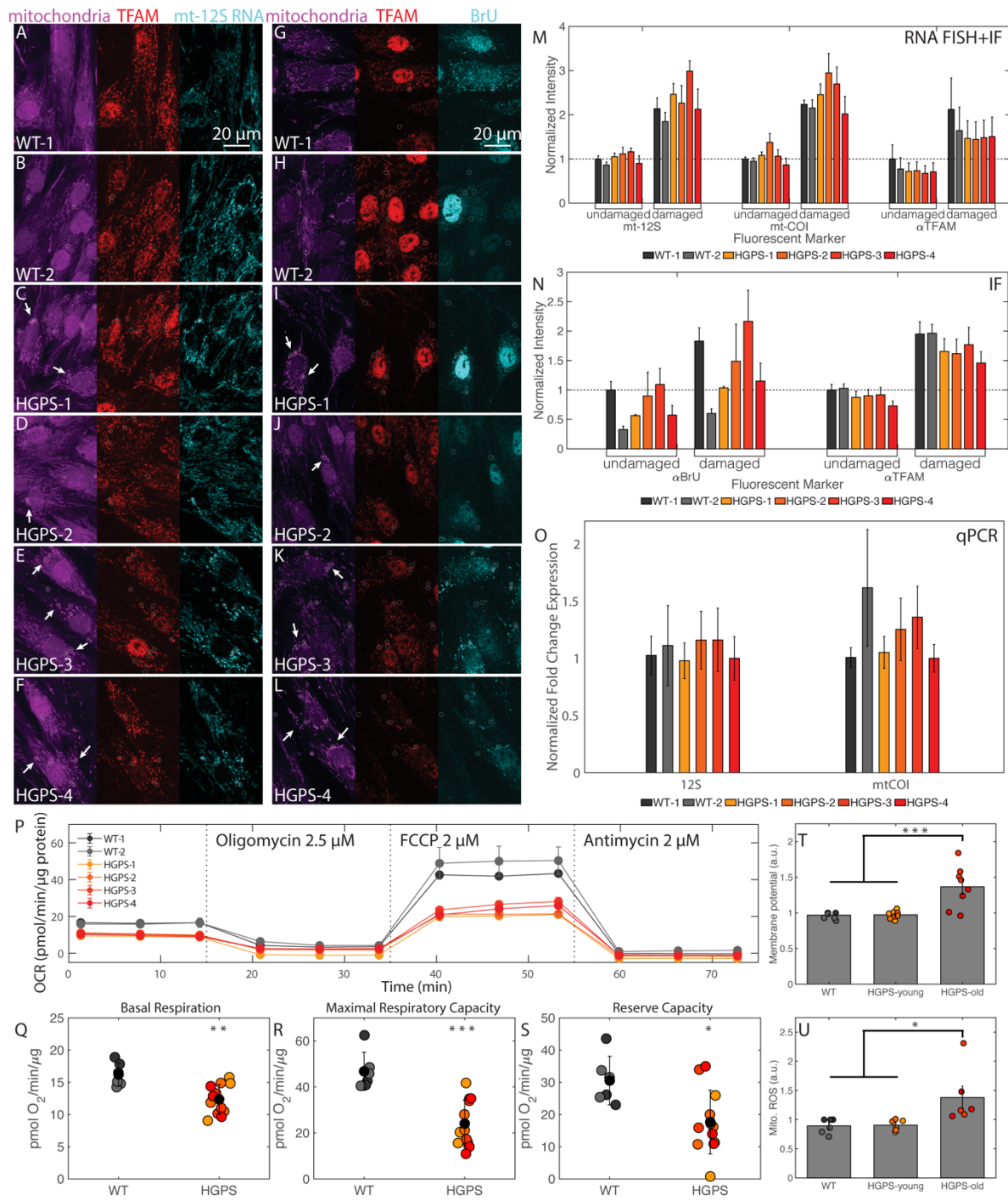
Appendix Figure S5: (A) FRAP recovery as a function of time on TFAM-mKate2 in live HeLa cells (n=20 cells, error bars represent standard deviation). For these experiments, bleaching (dashed circle) was performed on small nucleoids as to bleach the entire structure. (B-D) Images from FRAP experiment, showing pre-bleach (B), bleach (C), and post-bleach after 3.3 minutes (D). Images are an overlay of TFAM-mKate2 (red) and PicoGreen (green). Dashed circle indicates which nucleoid was bleached. Scale bar = 1 μm . (E) The same images as in Fig. 4C, except the intensity of only the TFAM-mKate2 channel is shown using a hot heatmap. (F-G) High-throughput confocal images of HeLa cells (F) and HeLa cells over-expressing a TFAM-mKate2 construct (G), where (n= 1 experimental replicate, with 3 technical replicates each with 16 fields of view). Cells were labelled as anti-TFAM (cyan), TFAM-mKate2 (red), anti-DNA (green), and MitoTracker Deep Red (magenta). Scale bar = 25 μm . (H-I) Images of mitochondria (MitoTracker Deep Red, magenta), TFAM (TFAM-mKate2, red), and mtDNA (PicoGreen, green) in HeLa cells in normal media (H) and hypotonic media (water) (I). Arrow heads point to nucleoids that remain as discrete structures in swollen mitochondria. Scale bar = 10 μm . (J) Single z-slice of a SIM image of enlarged nucleoids in fixed HeLa cells, where TFAM (TFAM-mKate2, red), mtDNA (anti-DNA, green), (anti-TFB2M, gray), and mitochondria (MitoTracker Deep Red, magenta) are labelled. Arrow points to swollen mitochondria with nucleoids occupying a fraction of the mitochondrial matrix. Scale bar = 10 μm .

Appendix Figure S6:



Appendix Figure S6: (A) SIM maximum intensity projection of a fixed HeLa with the nucleus (DAPI, blue), mitochondria (MitoTracker Deep Red, magenta), mtDNA (anti-DNA, green), and TFAM (TFAM-mKate2, red) from which nucleoids were shown in Fig. 5A-C. Scale bar = 5 μm . White boxes indicate nucleoids that were chosen for panels in A-C and in Fig. 5. (B,C) Single z-slices of SIM images in wild-type HeLa cells (B) or after over-expression of un-tagged TFAM (C). HeLa cells were labelled with anti-DNA (green) or anti-TFAM (red). Scale bar = 0.5 μm . For B-C, the intensity of the green channel is matched across all conditions, and the intensity of the red channel is matched for B and the first row of C, while the middle and bottom rows of C were significantly brighter and had different contrast settings applied. (D-I) Single z-slices of SIM images of nucleoids after over-expression of mutants in HeLa cells, including HMGA-mKate2 (D), HMGA+linker-mKate2 (E), $\Delta\text{C-tail-mKate2}$ (F), $\Delta\text{HMGA-mKate2}$ (G), L6-mKate2 (H), and no-dimer-mKate2 (I). Left most panel is of mtDNA (anti-DNA, cyan), followed by the mutant (mKate2, magenta), TFB2M (anti-TFB2M, yellow), and merged images. Scale bar = 0.5 μm . (J,K) Integrated intensity of mKate2 signal (J) or anti-DNA signal (K) from the single z-slice analyzed as a function of mt-nucleoid cross-sectional area ($A = \pi r^2$) for all mt-nucleoids analyzed ($n=20-40$ mt-nucleoids for each mutant construct). Correlation coefficient (95% confidence interval) is listed. Slope of 1 indicates proportional scaling between integrated intensity and area. (L) Average radius of all the nucleoids analyzed for TFAM variants ($n=20-40$ mt-nucleoids, error bars = s.d.). (M-O) Normalized correlation coefficients (correlation coefficient for each mutant divided by the average correlation coefficient of that mutant, where $n=20-40$ mt-nucleoids for each mutant construct) as a function of mt-nucleoid volume for TFAM-mtDNA (M), TFAM-TFB2M (N), and mtDNA-TFB2M (O). Correlation coefficient (95% confidence interval) is listed.

Appendix Figure S7:



Appendix Figure S7: (A-F) Representative high-throughput confocal images of WT-1 (A), WT-2 (B), HGPS-1 (C), HGPS-2 (D), HGPS-3 (E), and HGPS-4 (F) cell lines. Left image is mitochondria (MitoTracker Red, magenta); center image is TFAM (anti-TFAM, red); right image is mt-12S rRNA (RNA FISH, red). Scale bar = 20 μm . (G-L) Representative high-throughput confocal images of WT-1 (G), WT-2 (H), HGPS-1 (I), HGPS-2 (J), HGPS-3 (K), and HGPS-4 (L) cell lines. Left image is mitochondria (MitoTracker Red, magenta); center image is TFAM (anti-TFAM, red); right image is of nascent transcripts after BrU incorporation (anti-BrdU, red). Scale bar = 20 μm . (M-N) Based on high-throughput imaging, integrated intensity values for markers for mt-12s rRNA and mt-COI RNA (M) or BrU (N) along with anti-TFAM (M-N) were compared for nucleoids from undamaged and damaged (indicated by white circles in earlier images) mitochondria per cell and averaged, where $n=3$ experimental replicates and error bars represent standard error. (O) qPCR results for mitochondrial transcripts 12S and mt-COI for all cell lines. $n=3$ independent experimental replicates, each with three technical replicates, and error bars represent standard error. (P-S) Seahorse assay results on primary skin fibroblasts from wildtype cell lines (WT-1,2) and HGPS cell lines (young HGPS:1,2; old HGPS: 3,4) from a representative experiment. (P) The oxygen consumption rate (OCR) as a function of time after perturbation with oligomycin, 2.5 μM at $t = 16$ min, FCCP at 2 μM , at $t = 24$ min, and antimycin 2 μM at $t = 55$ min. Representative trace from a single experiment, error bars are SEM of technical replicates ($n=3$). Results measured from individual cell lines were pooled together (WT = WT-1,2 and HGPS = HGPS-1,2,3,4): basal respiration (Q), maximal respiratory capacity (R), and reserve capacity (S). Error bars represent standard deviation, where $*p<0.05$, $**p<0.01$ and $***p<0.001$. For (P), three experimental replicates were performed, and for (Q-S), experiments were pooled among cell types, where values represent averages \pm SD from $n = 6$ independent experimental replicates of WT cells and $n = 12$ independent experimental replicates of HGPS cells. (T) Mitochondrial membrane potential using TMRM. Results measured from individual cell lines were pooled together: WT (WT-1,2, $n=8$ independent measurements), HGPS young (HGPS-1,2, $n=8$ independent measurements), and HGPS old (HGPS-3,4,

n=8 independent measurements). Error bars represent SEM, where p-value for the ANOVA test statistic was $p < 0.001$. For individual pairs, $***p < 0.001$. (U) Mitochondrial ROS using MitoSOX Red. Results measured from individual cell lines were pooled together: WT (WT-1,2, n=6 independent measurements), HGPS young (HGPS-1,2, n=6 independent measurements), and HGPS old (HGPS-3,4, n=6 independent measurements). Error bars represent SEM, where p-value for the ANOVA test statistic was $p < 0.05$. For individual pairs, $*p < 0.05$.